production the absorptive peripheral model gives no reasonable results, but for $K^*(890)^{0,-}$ production the exchange mechanism can be determined using the model. The results agree well with the observed $K^*(890)^{0,-}$ production and decay angular distributions. Pion exchange is the dominant mechanism in production of $K^*(890)^0$ while ω exchange is dominant for $K^*(890)^-$ production.

The $K^*(1400)^{0,-}$ production and decay angular distributions suggest that the spin parity of the $K^*(1400)$ is 2^+, but without many more events or a better model for the production mechanism we cannot make a decisive determination. A better theoretical model would permit a quantitative use of the production angular distributions for $K^*(1400)^0$ and $K^*(1400)^-$ to help determine the spin-density matrix elements. This would then place more restrictions on the decay angular correlations so that a more definite distinction could be made between the distributions expected for different spin states.

The $K^*(1400)^0$ decay into $K\pi\pi$ appears to proceed entirely through $K^*(890)\pi$ and $K\rho$. The rates observed are in agreement with the $SU(3)$ predictions which assume that the $K^*(1400)$ is a member of a 2^+ octet.

ACKNOWLEDGMENTS

The experiment was made possible by the participation of our colleagues at the Universities of Illinois and Wisconsin in the design, construction, and operation of of the separated beam. In addition we wish to thank the ZGS and 30-in. bubble chamber staff for cooperation under conditions which were often difficult. Finally we thank our scanners both at Argonne and Northwestern for their careful work over an extended period.

PHYSICAL REVIEW VOLUME 166, NUMBER 5 25 FEBRUARY 1968

Positron-Proton Elastic Scattering at 800 and 1200 MeV*

R. L. Anderson,† B. Borgia,‡ G. L. Cassiday, J. W. DeWire, A. S. Ito, and E. C. Loh
Laboratory of Nuclear Studies, Cornell University, Ithaca, New York
(Received 15 September 1967)

The cross section for the elastic scattering of positrons from protons has been compared with the corresponding electron cross section using secondary beams derived from the photon beam of the Cornell 2-GeV synchrotron. The paths of the scattered leptons (positrons or electrons) and recoil protons were recorded in spark chambers and were used to determine the incident lepton energy of each event. Elastic scatterings were identified by requiring coplanarity and a fit to the scattering kinematics. The detection system was sensitive to scattering angles between 25° and 75°. The ratio of the positron cross section to the corresponding electron cross section was 0.992 ± 0.017 at 800 MeV and 0.987 ± 0.019 at 1200 MeV. No significant variation of the ratio with angle of scattering was found.

INTRODUCTION

A COMPARISON of the elastic scattering of positrons from protons with the well-known electron-proton process could be a sensitive test for the presence of two-photon exchanges in the interaction. At present, the large quantity of data on the absolute cross section for electron-proton scattering can be understood in terms of only single-photon exchanges, which lead to the Rosenbluth formula[1] for the scattering cross section. While it is true that the exchange of more than one photon should lead to a deviation from the Rosenbluth formula, the detection of such a deviation is made difficult by the need to make accurate absolute cross sections for comparison with the theory. The most accurate test of the well-known $\cot^2(\frac{1}{2}\theta)$ dependence of the scattering cross section, predicted by the Rosenbluth formula, is in excellent agreement with the theory.[2] A direct comparison of the positron-proton and electron-proton scattering rates for identical kinematic limitations is not subject to some systematic errors associated with absolute determinations. Furthermore, interference terms between one- and two-photon exchange processes, which depend on the sign of the leptonic charge, have an effect on the ratio of cross sections which is twice the effect on each cross section.

Two-photon exchange processes may also produce a linear polarization of the recoil proton, but the degree of polarization is proportional to the imaginary part of the amplitude for two-photon exchange while the contribution to the cross section comes from the real part of the amplitude. Experimental measurements have

* Supported in part by the U. S. Office of Naval Research and the National Science Foundation.
† Present address: Stanford Linear Accelerator Laboratory, Stanford, Calif.
‡ Present address: Instituto di Fisica, Universita di Roma, Rome, Italy.
[1] M. N. Rosenbluth, Phys. Rev. **79**, 615 (1950).
[2] W. Albrecht, H. J. Behrend, F. W. Brasse, W. Flauger, H. Hultschig, and K. G. Steffen, Phys. Rev. Letters **17**, 1192 (1966).

shown that the polarization if present is smaller than 5%.[3–5]

Two experiments to study positron-proton scattering have been reported in the literature.[6,7] Both were done at the Stanford Mark III Linac and together they included measurements for incident energies between 200 and 850 MeV and for laboratory scattering angles between 30° and 100°. The 12 measured ratios of the positron-proton and electron-proton cross sections when plotted against the square of the four-momentum transfer show a tendency to rise from a value of unity at $q^2=0$ to about 1.05 at $q^2=0.8(\mathrm{BeV}/c)^2$. However, no single point lies more than two standard deviations from unity. The most accurate data from these experiments came from measurements in which only the scattered leptons were detected in a magnetic spectrometer. In some cases, particularly at high momentum transfer, counts due to pions could not be completely distinguished from lepton counts, and sizeable corrections were made to account for this. The experiment reported in this paper represents an attempt to measure the ratio of cross sections while holding to a negligible level the detection of processes other than the interaction of the incoming leptons with the target protons.

POSITRON BEAM

The leptons (positrons or electrons) were produced by pair production in a lead radiator in the photon beam of the Cornell 2-GeV synchrotron. In order to keep the size of the source small, the radiator was placed 4 ft from the internal target of the synchrotron, in the fringe field of the synchrotron magnet. A laminated iron shield eliminated most of the field from the path of the charged pairs.

A system of five magnets produced an image of the pair source with unit magnification after selecting either positrons or electrons in a momentum interval of 10%. The distance between source and image was approximately 25 ft. A schematic diagram of the system is shown in Fig. 1, and the design parameters of the magnets are given in Table I. The magnets were excited in series and were mounted on a common beam which could be rotated about a vertical axis through the center of the first bending magnet, thus varying the deflection of the beam in both bending magnets. The beam aperture through the system contained helium at atmospheric pressure. The modest requirement on momentum resolution could be met by rather small magnets. Each was roughly a cube of edges

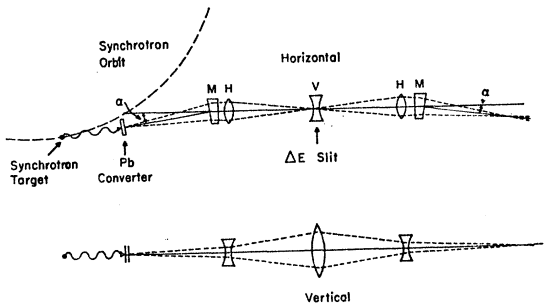

FIG. 1. Schematic diagram of the lepton beam transport system. The angle α was 0.060 rad. The distance between the lead converter and beam focus was 25 ft.

1 ft long. The water-cooled windings were made of $\frac{1}{4}$-in. copper tubing, permitting a current of 425 A which corresponded to a central momentum of 1200 MeV/c.

The minimum image size was found empirically by making small variations in the bending angle and in the current through the horizontal focusing quadrupoles. The latter adjustment was made by the use of simple water-cooled shunts made of thin stainless-steel tubing. The best image was $\frac{1}{4}$ in. wide and $\frac{3}{8}$ in. high, essentially independent of the momentum above 800 MeV/c. The linear dimensions of the image were doubled when the helium in the system was replaced by air.

The yield of leptons was measured as a function of the thickness of the lead radiator, and as expected showed a very broad maximum at about one radiation length when the lepton momentum was close to the momentum of the electrons in the synchrotron. For all our measurements a radiator of one-half radiation length was used. For a lepton momentum of 1200 MeV/c and a synchrotron maximum energy of 1400 MeV, the yield was 2×10^{-3} lepton per effective quantum in the photon beam. The measured momentum spread of the beam is shown in Fig. 2.

DETECTION SYSTEM

The scattering target was a cylinder of liquid hydrogen 18 in. long by $1\frac{1}{4}$ in. diameter. The center of the target was located at the focus of the lepton beam, and its axis was aligned with the beam. The hydrogen was contained in a 10-mil-wall stainless-steel tube with 1-mil stainless-steel end windows. A second 10-mil-wall tube of $1\frac{1}{2}$ in. diameter served as the outer wall of the insulating vacuum. The target was used in the manner de-

TABLE I. Parameters of magnets in beam transport system.

Magnets[a]	Over-all dimensions ($L\times W\times H$) (in.)	Gap height	Turns per pole
M	12×12×10	1 in.	16
H	10×12×12	$xy=(0.75\text{ in.})^2$	12
V	12×12×12	$xy=(1\text{ in.})^2$	12

[a] The nomenclature for the magnets is given in Fig. 1.

[3] J. C. Bizot, J. M. Buon, J. Lefrançois, J. Perez y Jorba, and Ph. Roy, Phys. Rev. Letters **11**, 480 (1963).
[4] J. C. Bizot, J. Perez y Jorba, D. Treille, University de Paris, École Normale Supérieure Laboratoire de l'Accelerateur Lineaire Report No. 1139, Orsay, France (unpublished).
[5] G. V. Di Giorgio, E. Gannssauge, R. Gomez, G. Gorini, S. Penner, S. Serbassi, M. L. Vincelli, E. Amaldi, and G. Stoppini, Nuovo Cimento **39**, 474 (1965).
[6] D. Yount and J. Pine, Phys. Rev. **128**, 1842 (1962).
[7] A. Browman, F. Liu, and C. Schaerf, Phys. Rev. **139**, B1079 (1965).

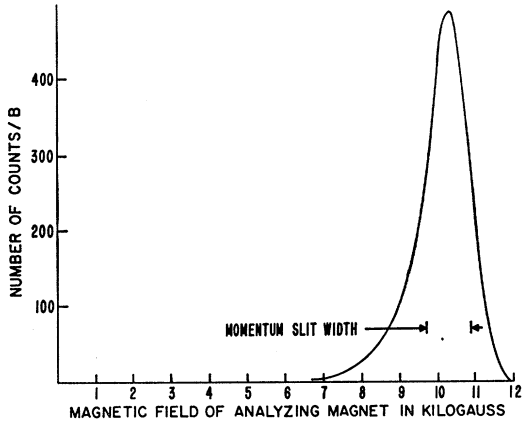

FIG. 2. Magnetic analysis of the incident beam. The width of the energy slit in the beam transport system was set to give 10% resolution for a point source.

scribed by Littauer.[8] The boil-off rate was approximately 130 cc liquid per hour.

The detection system covered the interval of scattering angles between 25° and 75° and scattering planes which departed from horizontal by as much as 20°. Elastic scattering was identified by observing the tracks of the scattered lepton and recoil proton in pairs of spark chambers placed symmetrically on both sides of the beam line. Choice of an elastic event was made by requiring that the two tracks lie in a plane containing the beam line and that the energy of the incident lepton, calculated from the scattering and recoil angles, agree with the known energy. In order to reduce the effect of multiple scattering of the proton and to minimize the probability of materializing a photon, the spark chambers were exposed directly to the hydrogen target. The trigger counters were placed behind the chambers.

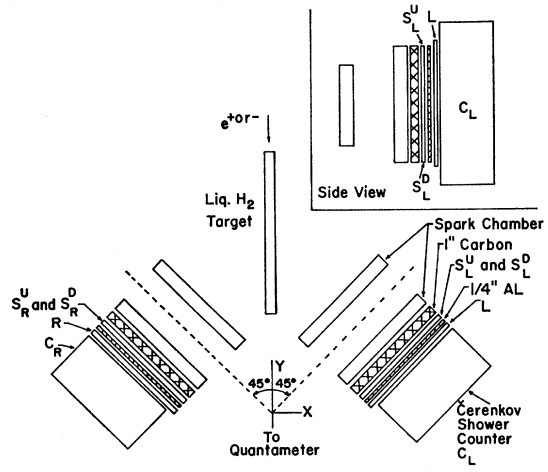

FIG. 3. Schematic diagram of the detection system. The insert shows a side view of one set of spark chambers and counters. S, L, and R are scintillation counters. C_L and C_R are Čerenkov shower counters.

A schematic view of the detection system is shown in Fig. 3. Behind each pair of chambers, there was a scintillation counter telescope and a lead-glass Čerenkov shower counter. Each telescope was a two-counter system with carbon and aluminum absorbers to exclude coincidences from protons of energy less than 100 MeV in the 800-MeV run and 150 MeV in the 1200-MeV run. The front counter of each telescope was split at the median plane into two counters as shown in the insert in Fig. 3. A scattered lepton produced a triple coincidence involving two scintillation counters and a Čerenkov counter; a recoil proton, and a double coincidence of two scintillation counters. Any one of the coincidences $S_R{}^D RC_R S_L{}^U L$, $S_R{}^U RC_R S_L{}^D L$, $S_L{}^D LC_L S_R{}^U R$, and $S_L{}^U LC_L S_R{}^D R$ was used to trigger the spark chambers. In addition, coincidences $S_R{}^D RC_R S_L{}^D L$ and $S_L{}^U LC_L S_R{}^U R$ were recorded to monitor the combined rates of inelastic events and accidentals. All scintillation counters were biased to count minimum ionizing particles. The Čerenkov counters were biased to count at least 90% of 400-MeV leptons in the 800-MeV run and 600-MeV leptons in the 1200-MeV run.

The aperture for recoil protons was a 13-in. square located 3 ft from the center of the target. For the scattered leptons the aperture was a 13-in. by 12-in. rectangle located $3\frac{1}{2}$ ft from the target. The active area of the spark chambers covered both trigger apertures for particles originating at any point in the target.

Each of the four spark chambers had four $\frac{3}{8}$-in. gaps separated by 2-mil aluminum foils stretched over glass frames. The exterior faces were covered with 5-mil Mylar foils. The chambers contained a gas mixture of 80% neon and 20% helium at atmospheric pressure.

The lepton beam was monitored by a quantameter[9] and in addition, during part of the experiment, by a thin-wall ionization chamber.

Stereoscopic views of the sparks were recorded on single frames of 35-mm film. A code number identifying which combination of counters triggered the chambers was also recorded, enabling us to distinguish the scattered lepton from the recoil proton. For each event, the pulse heights in both Čerenkov counters and four scintillation counters were recorded on a multidimensional pulse-height analyzer.[10] A serial number appearing on the spark-chamber film and the pulse-height print-out made it possible to correlate the pulse heights with the information obtained from the spark chambers.

The spark-chamber pictures were scanned and measured manually. They were projected by a modified Recordak film reader onto a template which could be aligned with the projected fiducial marks. In all pictures in which at least one track appeared on each side,

[8] R. M. Littauer, Rev. Sci. Instr. **29**, 178 (1958).

[9] R. R. Wilson, Nucl. Instr. Methods **1**, 101 (1957).

[10] R. M. Littauer and L. Tepper, Nucl. Instr. Methods **26**, 285 (1964).

TABLE II. Summary of raw data.[a]

Energy	Integrated beam (10^{12} leptons)	Triggers	Pictures scanned	Elastic events
1200 MeV—Run 1	1.387, 1.451	14846, 15334	7492, 7504	2625, 2636
1200 MeV—Run 2	2.160, 2.094	14349, 13470	13440, 12690	4245, 4053
800 MeV	1.067, 1.033	9532, 9061	9158, 8614	5542, 5295

[a] The number on the left in each column represents the positron data, the number on the right, the electron data.

every track was measured by laying a straight line over it and reading two points on appropriate scales. The data for all combinations of track pairs were punched on cards for computer processing. The scanning rate was approximately 200 events per day.

EXPERIMENTAL DATA

The data were collected in two runs at 1200 MeV and one at 800 MeV and are summarized in Table II. During each run the beam was alternated frequently between positrons and electrons in order to minimize the effect of long-term drifts in the apparatus. Conditions for the two runs at 1200 MeV were essentially identical except the biases on the Čerenkov counters. An analysis of 10% of the data from the first run showed that the biases could be increased without losing elastic scattering events, thereby eliminating a significant number of inelastic events in which a pion was detected in a Čerenkov counter. The remaining 90% was then limited to events corresponding to the higher bias, selected by using the recorded pulse heights. During the second run, the biases were set slightly lower than the cutoff used in the analysis of the first run.

The cards containing all possible pairs of tracks were run through a computer program by which the following quantities were found: location of the origin of each pair, angle between the horizontal plane and the plane determined by each track and the beam line, dihedral angle between the scattering and recoil planes, polar angle of each track, the energy of the incident lepton, and the square of the four-momentum transfer. The last two quantities are computed from the scattering and recoil angles of each pair of tracks using the kinematics of elastic scattering. For events whose triggers included pulses from both Čerenkov counters (about 10% of the total), the energy particle was the scattered lepton. The output data from this computation were treated by a second computer program in which frequency distributions against all variables were prepared for all events and for those selected within the limits placed on the variables.

In Figs. 4 and 5, typical plots of the distributions of the origins of all events for the second 1200-MeV run are shown. The distributions for positrons and electrons are superimposed for direct comparison. The horizontal beam width x calculated from the data is larger than that obtained from Poloroid film exposed directly in the lepton beam. This is a measure of the resolution of the spark chamber system. This is evident from the plot in Fig. 6 showing the distribution of events plotted

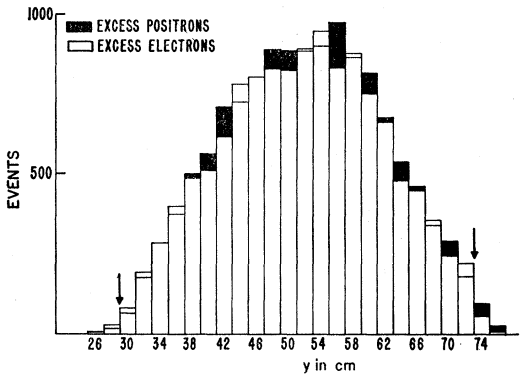

FIG. 5. Plot showing the locations of the origins of 1200-MeV track pairs along the incident beam line. The arrows marking the accepted events correspond to the edges of the target.

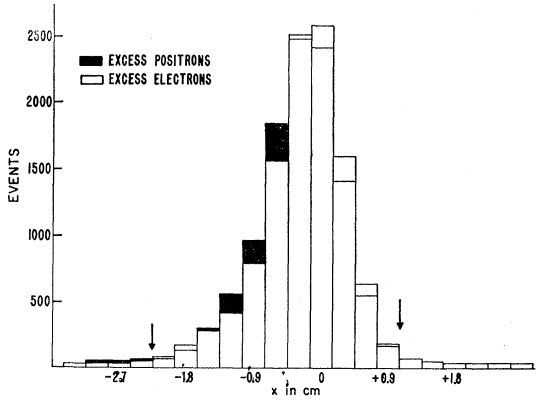

FIG. 4. Distribution of 1200-MeV event origins plotted against the distance x from the lepton beam line. Positron and electron data are superimposed. The arrows mark the interval of accepted track pairs.

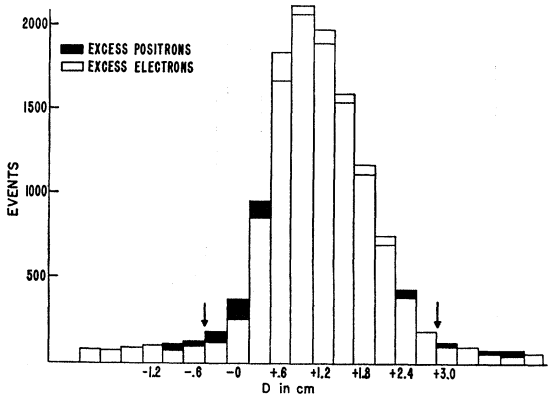

FIG. 6. Plot of the vertical separation of track pairs at the point of intersection of their projections on a horizontal plane. The width of the peak is a measure of the spatial resolution of the spark-chamber system.

against the vertical track separation where their projections on a horizontal plane crossed. The arrows on the plots mark the limits used in selecting track pairs which originated in the target. Variations of these limits and those in all other distributions did not produce significant changes in the final results.

Elastic events were selected in the manner illustrated by the plots shown in Figs. 4–8. The plots include the data from both runs at 1200 MeV, the numbers of positrons and electrons being normalized to the same exposure. Corresponding plots for the 800-MeV data are similar to those shown except for a somewhat reduced background of inelastic events. All events coming from the target are plotted in Fig. 7 as a distribution in angle of departure from coplanarity. The angle $\Delta\beta$ is the dihedral angle between the plane determined by the incident beam and scattered lepton and the plane determined by the beam and recoil proton. The width of the central peak is a measure of the resolution of the spark-chamber system. The smooth background of track pairs which are not coplanar is the same for positrons and electrons, and has a variation with $\Delta\beta$ which is what is expected for events uniformly spread in $\Delta\beta$ and selected by the finite detection apertures. The equality of the two backgrounds assures us that the final results are not biased by unequal contaminations by inelastic processes from positrons and electrons.

The coplanar events which are selected within the limits shown by the arrows in Fig. 7 are plotted in Fig. 8 against the incident energy, which is computed from the track polar angles using the relation

$$E=Mc^2(\cot\tfrac{1}{2}\theta\cot\phi-1),$$

where θ and ϕ are the scattering and recoil angles and M is the proton mass. This expression is good for energies large compared to the electron rest energy.

The low-energy tail in Fig. 8 can be understood as the sum of three approximately equal contributions:

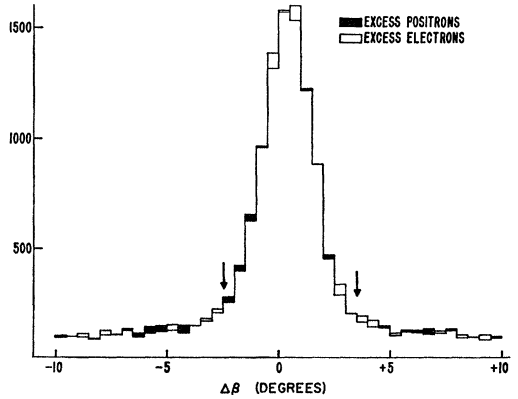

FIG. 7. Distribution plot to show the departure from coplanarity of all 1200-MeV track pairs which originate in the target. The angle $\Delta\beta$ is the dihedral angle between the plane determined by the incident beam and the scattered lepton and the plane determined by the recoil proton.

(1) Elastically scattered low-energy leptons: The number of leptons in the low-energy tail of Fig. 2 is small but is weighted by the scattering cross section which rises steeply as the energy decreases.

(2) Radiative scattering of leptons of the correct incident energy.

(3) Other inelastic events which by chance are coplanar: These and the radiative scatterings appear in the background under the peak in Fig. 7.

If we select events in the energy interval shown in Fig. 8 before making a coplanarity plot, the result shown in Fig. 9 is obtained. The effect of first choosing events of the proper energy is to reduce the inelastic background relative to the central peak by a factor of 2.5.

The events which have been selected for the correct incident energy and for coplanarity are plotted against the square of the four-momentum transfer in Fig. 10. A similar plot for the 800-MeV data is shown in Fig. 11.

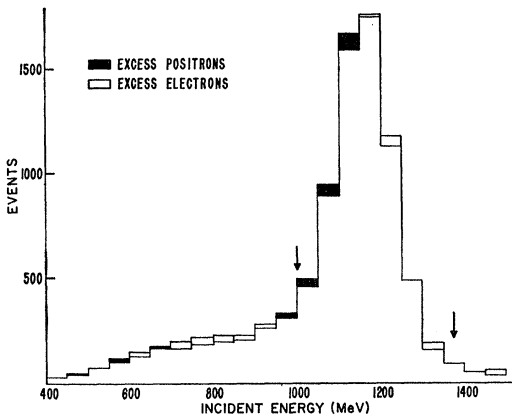

FIG. 8. Distribution plot of calculated incident energies of the 1200-MeV events within the interval show in Fig. 7. The origin of the low-energy tail is discussed in the text.

From these plots the uncorrected ratios of the cross sections for positrons and electrons are obtained. The ratio R is computed using the expression

$$R=\Delta\sigma^+/\Delta\sigma^-,$$

where for each $\Delta\sigma$ we evaluate

$$\Delta\sigma=\frac{\text{selected events}}{\text{incident leptons}}\times\frac{\text{triggers}}{\text{pictures scanned}}.$$

The uncorrected ratios are given in the third column of Table III for all events at each energy and for arbitrarily chosen intervals of q^2. The errors listed are statistical errors.

CORRECTIONS AND ERRORS

The equality of the inelastic backgrounds for positrons and electrons indicates that the influence of these events on the ratio of the elastic scattering cross sec-

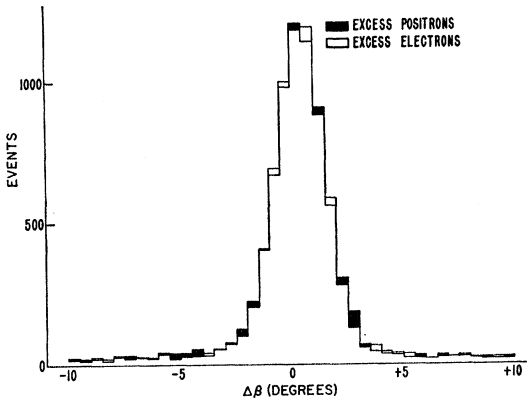

FIG. 9. Coplanarity plot of 1200-MeV events selected within the energy interval shown in Fig. 8. A comparison of this plot with the plot in Fig. 7 shows the reduction of the background achieved by the energy selection.

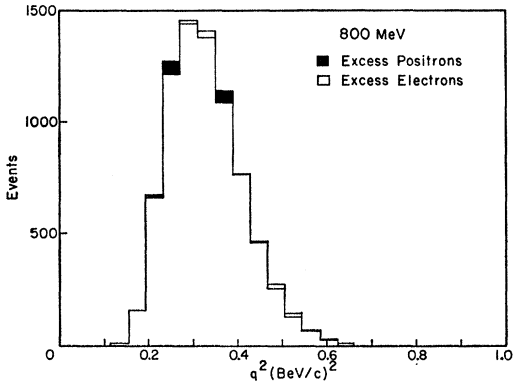

FIG. 11. Distribution of 800-MeV elastic events, plotted against q^2.

tions is small. Electroproduction of pions should be equally probable for positrons and electrons. Photoproduction of neutral pions can contribute to the inelastic background, possibly in different amounts for positrons and electrons through annihilation radiation and bremsstrahlung from collimators. We have estimated this contribution to the background by counting events where the system is triggered by conversion of a photon in the first scintillator thus leaving no track in the spark chambers on the lepton side of the detector. The contribution to the background is about 1% and approximately equal for positrons and electrons.

Elastic pion-proton scattering can contribute to the coplanar events because the kinematic angles differ from those for lepton-proton scattering by less thna 0.5° at these energies. Pion scattering can be distinguished from lepton scattering only by the pulse heights in the Čerenkov counters, but the resolution of the counters is not sufficient to separate completely the two processes. However, from the known cross sections for charged-pion photoproduction in nuclei[11,12] and for pion-proton elastic scattering[13,14] we estimate that this process would contribute less than one event for 10^4 lepton scatterings if the Čerenkov counters detected all scattered pions. Direct evidence that pion scattering was not detected came from an analysis of the events with small Čerenkov pulse heights in the first 1200-MeV run. In this sample no coplanar event was found above background.

A correction must be made for those scatterings which are not detected because the interacting particles radiate photons and fall outside the kinematic limits for selecting elastic events. For this experiment only the term corresponding to interference between radiation by the lepton and proton need be considered. The correction has been calculated from the term proportional to Z in Eq. (3.23) of the paper by Yennie, Frautschi, and Suura.[15] Included in this calculation is the effect of virtual two-photon exchange for which there is an infrared divergence. The imposed limits on incident energy and coplanarity determine the extent of the phase space of radiated photons corresponding to undetected events. The corrections to the ratio of cross sections were found to be nearly independent of

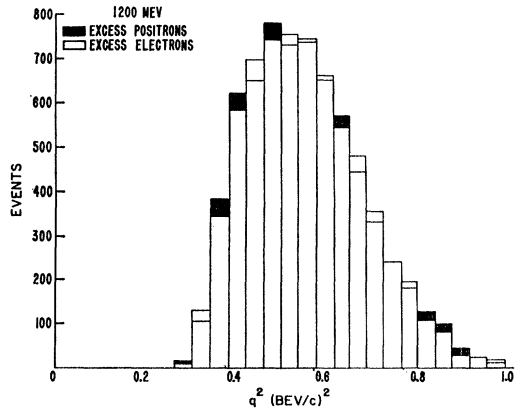

FIG. 10. Distribution of elastic scattering events, plotted against the square of the four-momentum transfer. All 1200-MeV data are plotted.

TABLE III. Summary of experimental results and corrections.

Incident energy (BeV)	q^2 (BeV/c)²	Measured R	Radiation correction	Energy correction	Corrected R
0.80	All events	1.008±0.016	−0.014	−0.002	0.992±0.017
	0.15−0.31	1.021±0.024	−0.014	−0.016	0.991±0.024
	0.31−0.62	0.997±0.022	−0.014	+0.009	0.992±0.022
1.20	All events	1.017±0.018	−0.022	−0.008	0.987±0.019
	0.27−0.54	1.049±0.025	−0.022	−0.013	1.014±0.025
	0.54−0.70	0.991±0.029	0.022	−0.001	−0.968±0.029
	0.70−1.00	0.987±0.044	0.022	+0.015	1.002±0.045

[11] W. A. Blanpied, J. S. Greenberg, V. W. Hughes, D. C. Lu, and R. C. Minehart, Phys. Rev. Letters **11**, 477 (1963).
[12] R. B. Blumenthal, W. L. Faissler, P. M. Joseph, L. J. Lanzerotti, F. M. Pipkin, D. G. Stairs, J. Ballam, H. De Staebler, Jr., and A. Odian, Phys. Rev. Letters **11**, 496 (1963).
[13] D. E. Damouth, L. W. Jones, and M. L. Perl, Phys. Rev. Letters **11**, 287 (1963).
[14] F. Bulos *et al.*, Phys. Rev. Letters **13**, 558 (1964).
[15] D. Yennie, S. Frautschi, and H. Suura, Ann. Phys. (N. Y.)**13**, 379 (1961).

q^2 for the interval covered by this experiment and are listed in the fourth column of Table III.

Another correction has been made to take into account a small difference in the incident energies of positrons and electrons, most probably caused by a residual field inside the magnetic shield at the synchrotron magnet. In the first run at 1200 MeV the energy difference was not significant, but the alignment of the beam collimators for the second run was such that the electrons had a slightly higher energy than the positrons, 0.5% at 1200 MeV and 0.3% at 800 MeV. The difference was first found in the analysis of the data and was confirmed by a magnetic analysis of the focused beam. The correction to the ratio of cross sections was determined by a computer calculation of the efficiency of the detection system for various incident energies. The error in this correction is no larger than 20% and does not contribute appreciably to the error in the final results.

Background data were taken with the liquid hydrogen removed from the target. For both positrons and electrons, the background rates were less than 0.25% of the elastic scattering rates.

Several sources of error other than the statistical error have been considered in determining the final experimental error. The stability of the quantameter is known to be of the order of 0.1% over a period of a day during which time the experiment was alternated between positrons and electrons several times. During the second run at 1200 MeV the stability was checked against the response of a thin-air ionization chamber in the lepton beam. The rms variation of the ratio of the readings on the two chambers was about 0.3%. It is probable that most of the variation took place in the thin chamber. Several contributions to scanning error were considered but were found to be negligible. Each scanner processed roughly equal quantities of positron and electron film. Samples of the film were analyzed to look for a significant difference in track frequencies or multiplicites but none was found. The error in the radiative correction is estimated to be about 15%. The total contributions to the errors in the final results, excluding the statistical errors, is thus approximately 0.5%.

RESULTS AND DISCUSSION

The corrected ratios of scattering cross sections are given in the last column of Table III. The ratios for all of the events at each incident energy are shown and also ratios for arbitrarily chosen intervals of q^2. From these numbers we can conclude that the average cross sections within the kinematic limits of the detection system are the same to an accuracy of about 2%. The cross-section ratios are plotted in Fig. 12 with the results of the previous experiments. The dependence of the ratio on q^2, which was indicated by the Stanford data, is not supported by our results. It is clear that no effect of a two-photon exchange can be seen in the data.

Calculations of corrections to the Rosenbluth formula fall into two categories, those dealing with

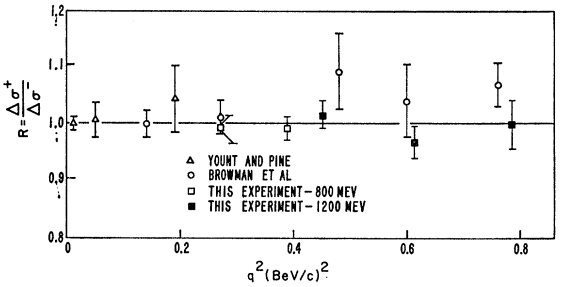

FIG. 12. Plot of experimental values of the ratio of the positron and electron scattering cross sections from protons. The points include the results of this experiment and the most accurate points from Refs. 6 and 7.

purely electrodynamic effects and others considering the influence of possible resonances on the two-photon exchange diagrams. The published electrodynamic calculations[16–19] have treated the proton as a static charge and do not directly apply to the present experiment in which the scattering is dominated by the interaction with the magnetic moment of the proton. Greenhut[20] has extended these calculations by including the effect of a static magnetic moment, using both the second Born approximation and a distorted-wave approximation.[21] He shows that for the kinematic conditions of this experiment the positron scattering should be roughly 0.5% higher than electron scattering, at 800 and 1200 MeV. Calculations of the effects of resonances[22,23] on the scattering cross sections have been carried out only to the extent of estimating the size of the correction and do not make definite predictions. It is expected that these corrections will also be somewhat less than 1%.

The experiments to date eliminate the possibility that two-photon exchange interactions play a larger role in electron-proton scattering than that predicted by present theories. Greater experimental accuracy will be required to provide a direct comparison with these theories.

ACKNOWLEDGMENTS

We wish to thank Professor R. R. Wilson who suggested this experiment and designed the magnets for the positron beam and Professor Martin Feldman who worked on preliminary studies. We also thank Anil Rae for computing the radiative corrections and Professor Donald Yennie for helpful discussions concerning the theory. We are grateful to Mary Johnson and Geraldine Jackson for their efficient handling of the bulk of the scanning. The generous cooperation of the operating crew of the Cornell synchrotron is also acknowledged.

[16] W. McKinley and H. Feshbach, Phys. Rev. **74**, 1759 (1948).
[17] R. Lewis, Phys. Rev. **102**, 537 (1956).
[18] S. Drell and R. Pratt, Phys. Rev. **125**, 1394 (1962).
[19] G. Bisiacchi and G. Furlan, Phys. Letters **3**, 186 (1963).
[20] G. Greenhut (private communication).
[21] D. R. Yennie, F. L. Boos, and D. G. Ravenhall, Phys. Rev. **137**, B882 (1965).
[22] S. Drell and S. Fubini, Phys. Rev. **113**, 741 (1959).
[23] N. Werthamer and M. Ruderman, Phys. Rev. **123**, 1005 (1961).